Journal of Power Sources 202 (2012) 1–10

Contents lists available at SciVerse ScienceDirect

Journal of Power Sources

journal homepage: www.elsevier.com/locate/jpowsour

High-performance direct methanol alkaline fuel cells using potassium hydroxide-impregnated polyvinyl alcohol/carbon nano-tube electrolytes

Shingjiang Jessie Lue[a,*], Wen-Han Pan[a], Chia-Ming Chang[b], Ying-Ling Liu[c,**]

[a] Department of Chemical and Materials Engineering, Chang Gung University, Kwei-shan, Taoyuan 333, Taiwan
[b] Department of Chemical Engineering, R&D Center for Membrane Technology, Chung Yuan University, Chungli, Taoyuan 320, Taiwan
[c] Department of Chemical Engineering, National Tsing Hua University, Hsinchu 30013, Taiwan

ARTICLE INFO

Article history:
Received 23 September 2011
Received in revised form 22 October 2011
Accepted 24 October 2011
Available online 3 November 2011

Keywords:
Cell performance
Nano-composites
Free volume
Conductivity
Operating conditions

ABSTRACT

This research focuses on improving direct methanol alkaline fuel cell (DMAFC) performance using hydroxide-potassium-doped polyvinyl alcohol/carbon nano-tube (PVA/CNT/KOH) electrolytes. The CNTs must be functionalized with PVA polymer chains to improve their dispersion in the polymer matrix and enhance the cell performance. A functionalized CNT load of 0.05% exhibits the highest cell voltage and power density among the PVA electrolytes containing 0–0.1% CNT. The cell voltage increases with the cell temperature between 30 and 60 °C. The open-circuit voltage and peak power density (P_{max}) are highest at 6 M KOH concentration in the anode feed. A methanol concentration of 2 M produces a higher P_{max} compared to concentrations of 1 M and 6 M methanol. The cell performance is enhanced by increasing the fuel flow rate into the anode. A P_{max} of 68.1 mW cm^{-2} is obtained for a DMAFC employing PVA/0.05%CNT/KOH electrolyte at 60 °C with 2 M methanol and 6 M KOH as the anode feed at a flow rate of 30 mL min^{-1} and humidified oxygen at a flow rate of 100 mL min^{-1} to the cathode. To the best of our knowledge, this P_{max} is the highest reported value in the literature for DMAFCs.

1. Introduction

Fuel cells constitute a potential energy resource that has received much attention in the last few decades. Although proton-exchange membrane fuel cells (PEMFCs) using hydrogen fuel have been studied extensively, direct methanol fuel cells (DMFCs) are considered suitable for portable and mobile devices. To date, overall DMFC cell performance has not achieved satisfactory voltage output. The high methanol crossover rate produced using perfluorosulfonic acid membranes, such as Nafion®, have resulted in fuel loss and reduced cell voltage [1–3].

To overcome the drawbacks of DMFCs, direct methanol alkaline fuel cells (DMAFCs) have been investigated throughout the last few years [4–10]. An informative review article has been published by Yu et al. [11]. The main advantages of the DMAFC include faster methanol oxidation kinetics in an alkaline media than in acidic solutions and the potential to use inexpensive non-precious metal catalysts [4,12]. In a DMAFC, an oxidant (air or oxygen) reacts with water to produce hydroxide ions at the cathode. The methanol fuel is oxidized into carbon dioxide and water by reacting with the hydroxide ions [7,8]. The hydroxide ions are transported through the membrane electrolyte along a direction opposing methanol flow, thus reducing methanol crossover. Some researchers have used liquid alkaline and anion-exchange membranes [4,6,13–18] as DMAFC electrolytes. However, the cell performance of the devices is lower than that of devices with alkaline-doped polymer electrolytes [10,19–23]. Among these polymer materials, polyvinyl alcohol (PVA) and its composites have rendered the highest power density [7,8,24]. Fillers such as fumed silica (FS) [7,8], chitosan [25], titanium oxide [26], alumina [9], carbon nano-tubes (CNTs) [27], and tetraethyl ammonium chloride [28] have been incorporated into PVA to generate new materials to improve the properties of the electrolyte. In our previous work, we reported that FS and PVA nano-composites can reduce methanol permeability and increase the fractional free-volume [8,29]. A KOH-doped PVA/FS electrolyte was observed to achieve a peak power density of 39 mW cm^{-2} using 2 M methanol and 6 M KOH at 60 °C [7].

Carbon nano-tubes (CNTs) have recently been considered as effective polymer fillers and have been incorporated into fuel cell polymer matrices. Pillai et al. demonstrated increases in proton conductivity with 0.05 wt% of sulfonated single-walled CNTs and 0.05 wt% sulfonated multi-walled CNTs (MWCNTs) in Nafion®-based membranes [30,31]. Liu et al. reported that 0.05 wt% Nafion®-functionalized MWCNTs increased the proton conductivity and improved DMFC performance using a Nafion®-based membrane. In DMAFC applications, Lue et al.

* Corresponding author. Tel.: +886 3 2118800x5489; fax: +886 3 2118700.
** Corresponding author. Tel: +886 3 5711450; fax: +886 3 5715408.
E-mail addresses: jessie@mail.cgu.edu.tw (S.J. Lue), liuyl@mx.nthu.edu.tw (Y.-L. Liu).

0378-7753/$ – see front matter © 2011 Elsevier B.V. All rights reserved.
doi:10.1016/j.jpowsour.2011.10.091

added 0.05 wt% PVA-functionalized MWCNTs into a PVA matrix and observed enhanced ionic conductivity and cell performance compared with pristine PVA. This PVA/CNT/KOH electrolyte achieved a peak power density of 39 mW cm^{-2} using 2 M methanol and 6 M KOH at 60 °C [24], a value similar to that attained with a PVA/20%FS/KOH electrolyte [7]. PVA/FS and PVA/CNT electrolytes have outperformed other DMAFCs in terms of power density and operating current density [7,24].

The objective of the present work was to study the effect of operating conditions on DMAFC performance using KOH-doped PVA and PVA/CNT composites. The cell temperature, fuel and oxygen flow rates, methanol concentration, KOH concentration, and CNT load effects on peak power density and current density are reported. The characteristics of the PVA/KOH and PVA/CNT/KOH electrolytes were also investigated and observed to correlate with the fuel cells' peak power densities.

2. Experimental

2.1. Materials

Multi-walled carbon nano-tubes (MWCNT) with average diameters of 10–50 nm and lengths of 1–25 μm were received from the Carbon Nano-tube Co., Ltd., Incheon, Korea. The purity of the received MWCNTs was 93%. The MWCNTs were washed with dimethylsulfoxide to remove impurities prior to use. Polyvinyl alcohol (PVA, average molecular weight of 89,000–98,000, more than 99% hydrolyzed) and potassium hydroxide (KOH) were obtained from Sigma–Aldrich (St. Louis, MO, USA). Methanol (HPLC grade, 99.9%) was obtained from Acros Organics, Geel, Belgium. A gas diffusion anode composed of 5 mg cm^{-2} Pt–Ru alloy (1:1) black and a gas diffusion cathode composed of 5 mg cm^{-2} Pt black were purchased from E-Tek (Somerset, NJ, USA). Pure water with a resistivity of 18 MΩ cm was produced using a Millipore water purifier (Elix 5/Milli-Q Gradient system, Millipore Corp., Bedford, MA, USA).

2.2. MWCNT functionalization with PVA

PVA-functionalized MWCNTs were prepared using an ozone-mediated method as reported previously [32–34]. In this process, PVA was dissolved in 30 mL water at 70 °C with a stirrer. The PVA solution was purged with ozone gas for 15 min. The PVA solution was then purged with argon gas for 15 min. The MWCNTs were then added to the PVA solution and stirred at 80 °C for 3 h to graft the PVA polymer onto the MWCNT. Finally, the functionalized MWCNTs were collected using a centrifuge, washed with hot water, collected using filtration, and dried over night. These PVA-functionalized MWCNTs are referred to as CNTs in the following sections, as apposed to the nascent MWCNTs (referred to as NCNTs).

2.3. Membrane and electrolyte preparation

The PVA film and PVA/CNT composites were prepared using a solution casting method described in our previous papers [24,35]. A predetermined amount of PVA-functionalized CNTs was suspended in 10 mL deionized water and added to a PVA aqueous solution (15 g polymer in 50 mL water) under ultra-sonication at room temperature. Another 75 mL of DI water was used to rinse the beaker wall and remove the remaining CNTs so that all CNTs were transferred to the PVA solution (total of 135 mL). The solution was heated to 90 °C under ultra-sonication and stirring (250 rpm) for 6 h. The homogenous suspension was cast onto a glass plate. A film with a uniform thickness (150 ± 30 μm) was obtained after drying in a vacuum oven at 60 °C for 6 h. The prepared membranes were denoted as PVA and PVA/CNT. The CNT content ranged from 0 to 0.1% (by weight) in the PVA matrix, and the composites are denoted as PVA/*x*CNT or PVA/*x*CNT/KOH for the films containing *x*% CNT. A similar procedure was followed to prepare the PVA/NCNT composite, in which the nascent, unmodified CNTs were mixed with PVA solution prior to film formation.

2.4. Positron annihilation lifetime spectroscopy

The free volume property of the wet and dry PVA and PVA/0.05CNT films was examined using the positron annihilation lifetime spectroscopy (PALS). A radioactive source was sandwiched between two stacks of tested film. The emitted positron entered the specimen and was annihilated within the PVA matrix. The generated positron and positronium were annihilated and localized in the region of low electron density, which is in the free volume of a polymer system. The *ortho*-positronium (*o*-Ps) annihilation lifetime reflects the free volume size, and the PALS spectrum was analyzed using MELT software to reveal the lifetime and free volume size distribution. The detailed procedure is reported in our previous publication [29]. Moistened films were prepared after equilibrating the PVA and PVA/CNT films in water vapor, and a similar PALS analysis was performed.

2.5. Characterization of alkali-doped PVA/CNT films

These membranes were immersed in KOH solutions (1, 2, and 6 M, the same concentration employed in the cell performance measurements) for at least 24 h before testing. These KOH-doped PVA and PVA/CNT polymer electrolytes were denoted as PVA/KOH and PVA/CNT/KOH, respectively. The alkali uptake (M) was calculated according to the following equation:

$$M = \frac{M_t - W_o}{W_o} \quad (1)$$

where W_o is the film dry weight and W_t is the total weight after being immersed in the KOH solution. The relative increase in film thickness (E) was measured using a thickness gauge (model 7331, Mitutoyo Co. Ltd., Kawasaki, Japan) before and after KOH immersion:

$$E = \frac{L_t - L_o}{L_o} \quad (2)$$

where L_o is the dry film thickness and L_t is the total thickness after being immersed in KOH solution.

The ionic conductivity of the KOH-doped electrolyte was determined by alternate current (AC) impedance using a potentiostat (Autolab, PGSTAT-30, Eco Chemie B.V., Utrecht, Netherlands). The electrolyte was sandwiched between two stainless steel electrodes, each with a surface area of 1.33 cm^2, in a spring-loaded glass T-holder [7]. This apparatus was maintained in a chamber with controlled relative humidity (>95%) and temperature (30–60 °C). The sample was scanned from 100 kHz to 100 Hz with a small voltage bias of 5 mV (e.g., in potentiostatic mode). The bulk resistance was determined from the Nyquist plot of the KOH-doped electrolytes according to the procedure described in the literature [7,24]. The conductivity (σ, in S cm^{-1}) of the KOH-doped electrolyte was calculated using the following equation:

$$\sigma = \frac{L_t}{R_b A} \quad (3)$$

where L_t is the thickness of the KOH-saturated electrolyte (cm), R_b is the bulk resistance (Ω), and A is the contact area of the stainless steel electrodes (cm^2) [7].

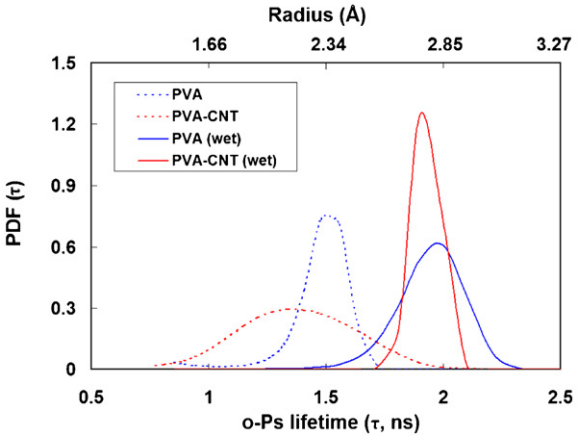

Fig. 1. *ortho*-Positronium (*o*-Ps) lifetime distribution probability density function (PDF) for dry PVA and PVA/0.05CNT (dash curves), and wet films (solid curves). The corresponding free-volume hole radius is shown in the upper *X*-axis.

2.6. Membrane electrode assembly and cell performance measurements

To prepare the hydroxide-conducting electrolytes used in the fuel cell test, the PVA and PVA/CNT films were doped with 6 M KOH, unless stated otherwise. The KOH-doped electrolyte was sandwiched between an anode gas diffusion electrode and a cathode gas diffusion electrode to prepare a membrane electrode assembly of 5 cm^2. Two flow-field plates made of high-density carbon with carved double-channel serpentine flow paths (1 mm wide and 1 mm deep) were fixed next to the MEA. Two gold-plated copper end plates were used as current collectors and were assembled next to the flow-field plates. The thermostated methanol/KOH solution was fed into the anode and humidified oxygen gas at room temperature was fed into the cathode. A detailed description was provided in our previous paper [7]. The KOH concentration for PVA composite doping was the same as that in the fuel feed to the anode of the DMAFC to avoid a fluctuation in the alkali concentration in the electrolyte and in the feed stream during fuel cell testing. The DMAFC cell voltage (V) was obtained by varying the current at 5-mA intervals and equilibrated for 7 s between intervals during the polarization curve measurement using an electrical load (PLZ164WA electrochemical system, Kikusui Electronics Corporation, Tokyo, Japan). The power density was calculated as the product of cell voltage and current density (I). The power density was plotted against the current density (P–I curve) to determine the peak power density (P_{max}) in the tested current density range. The cell performance of the DMAFC was investigated as a function of the CNT functionalization and load (0–0.1%), anode fuel flow rate (5–30 mL min^{-1}), oxygen flow rate (100–200 mL min^{-1}), methanol concentration (1–6 M), KOH concentration (2–8 M), and temperature (30–60 °C).

3. Results and discussion

3.1. PVA/CNT free volume and alkali uptake characteristics

The dry and moistened PVA and PVA/0.05CNT films were examined with respect to their polymer free volume property using PALS. The probability density function of the free volume size distribution is illustrated in Fig. 1. The dry PVA film exhibited an *o*-Ps positron annihilation lifetime of 1.5 ns, corresponding to a free volume radius of 2.34 Å. The dry PVA/CNT composites had a similar free volume but with a broader size distribution than the dry PVA. After these films were moistened, their free volume size grew to 2.7–2.8 Å. The wet PVA/CNT had a higher hole density than the wet PVA film, as indicated by the higher peak intensity in Fig. 1. This finding indicates that the PVA polymer free volume increased in both the PVA and PVA/CNT samples. Using differential scanning calorimetry (DSC), we previously demonstrated that the polymer crystallites were transformed into amorphous regions in the wet PVA sample [29]. In the current work, the PALS data show that CNT addition had a pronounced effect on the free volume upon solvation. This effect resulted in a higher number of free volume holes and an increase in polymer fractional free volume. This finding is in line with the decreased crystallinity, increased water diffusivity, and elevated conductivity (Table 1) in the PVA/CNT and PVA/CNT/KOH samples compared with the PVA counterparts in our previous report [24]. This increased polymer free volume is beneficial for water retention and hydroxide ion diffusion.

Table 1
Transport properties of PVA and PVA/0.05CNT and ionic conductivity of KOH-doped PVA films [24].

Property	PVA	PVA/0.05CNT
Water uptake (g g^{-1})[a]	2.81	2.94
Water diffusion coefficient (10^{-7} cm^2 s^{-1})[a]	2.14	3.09
Methanol permeability (10^{-7} cm^2 s^{-1})[b]	3.57	2.99
Ionic conductivity (10^{-2} S cm^{-1})[c]	10.88	11.76

[a] At 25 °C.
[b] At 1 M methanol and 30 °C.
[c] For 6 M KOH-doped samples at 60 °C.

The dry PVA/CNT films were immersed in 1–8 M KOH solutions for 24–72 h to ensure sorption equilibrium had been reached. The alkali uptake and increases in thickness of the PVA/CNT films in the KOH solutions are shown in Table 2. Both the alkali uptake and thickness of the PVA/0.05NT/KOH electrolyte showed little changes with the increase in the immersion time from 24 to 72 h. It was concluded that 24 h was sufficient to achieve alkali sorption equilibrium. The KOH solution uptake decreased from 2.82 ± 0.04 g g^{-1} to 1.08 ± 0.02 g g^{-1} with an increase in KOH concentration from 1 to 8 M. The thickness increases showed a decreasing trend (from $110 \pm 2\%$ to $75.5 \pm 6.9\%$ at 1–8 M KOH) similar to that of the KOH uptake.

3.2. Reproducibility measurement

The reproducibility of the V–I and P–I curves was determined using 1 M methanol and 6 M KOH at 60 °C using the varying current density mode of the electrical load. The data shown in Fig. 2 represent the largest variation in the cell performance carried out under the same operating conditions but with different MEAs on different days. The open-circuit voltage (V_{oc}) value was taken from the V–I curve by extrapolating the data for the low current density region (<5 mA cm^{-2}) to the y intercept (i.e., y value at $I = 0$). The experimental errors for the V_{oc} and P_{max} were 0.04 V and 0.80 mW cm^{-2}, respectively, corresponding to coefficients of variation of 4.9% and

Table 2
Alkali uptake and film thickness increase in PVA/0.05CNT/KOH electrolyte at 25 °C for various immersion times.

	Time (h)	KOH concentration				
		1 M	2 M	4 M	6 M	8 M
Alkali uptake (g g^{-1})	24	2.82	2.63	1.58	1.13	1.06
	48	2.79	2.53	1.53	1.18	1.09
	72	2.86	2.57	1.59	1.21	1.09
Thickness increase (%)	24	112.5	116.7	72.7	68.2	68.6
	48	108.3	100	77.3	77.3	75.6
	72	108.3	100	77.3	81.8	82.3

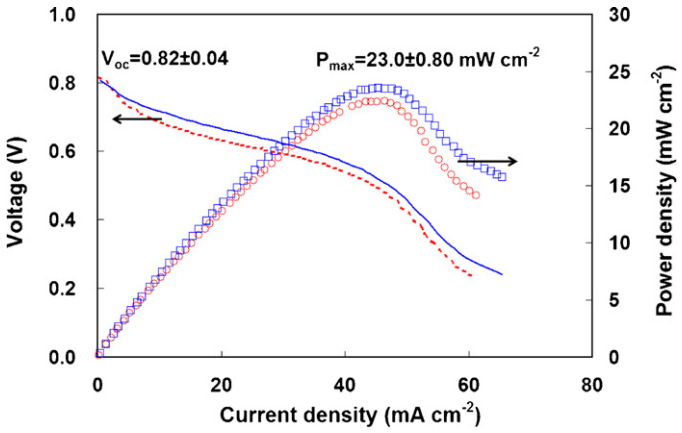

Fig. 2. Reproducibility of voltage and power density of DMAFC at 60 °C (anode: 1 M methanol in 6 M KOH with a flow rate of 5 mL min^{-1}, cathode: humidified oxygen with a flow rate of 50 mL min^{-1}).

3.5%. These results indicated that the cell performance measurement was very reproducible.

3.3. Effect of CNT functionalization on cell performance

Fig. 3 shows how the PVA functionalization affects the cell performance of PVA-based membranes at 30 and 60 °C. The investigated electrolytes consisted of PVA and the PVA composites containing CNT and NCNT. The V_{oc} ranged from 0.72 to 0.80 V at 30 °C and from 0.80 to 0.86 V at 60 °C using these electrolytes. The differences between the V_{oc} data at the same temperature were on approximately the same order as the experimental error. Therefore, the addition of 0.05% CNTs and the CNT functionalization had a limited impact on the V_{oc} under the tested operating conditions.

As the current density increased (especially beyond 10 mA cm^{-2}), differentiation in the cell potential became significant. The PVA containing 0.05% functionalized CNTs (PVA/0.05CNT) had the highest cell voltage and power density at both temperatures. The material containing the same amount of NCNTs had the lowest power density—even lower than that of the PVA/KOH electrolyte. The un-functionalized CNTs may have resulted in electron leakage between the electrode catalysts because NCNTs are good electron conductors [36]. This NCNT channel may have caused generated electrons to by-pass through the PVA/NCNT/KOH electrolyte instead of traveling along the external circuit. Therefore, the cell voltage of the DMAFC using the NCNT-containing PVA film was lower than that using the PVA film.

In contrast, the PVA/0.05CNT/KOH electrolyte exhibited higher cell performance than the PVA/KOH film. The CNT-containing electrolyte exhibited the lowest slopes in the ohmic over-potential region (Fig. 3) and was able to operate at a higher current density than the PVA and PVA/NCNT samples. The CNT surface was functionalized with PVA chains to increase its chemical compatibility with the polymer matrix for the film formation process. It may have enhanced the intrinsic ionic conduction after alkali doping because CNTs were wrapped at a nanometer thickness by KOH-doped PVA [24], which functioned as a hydroxide-conductive path [37]. The CNT core was insulated by the polymer wrapping, and the electron leakage could be minimized. Moreover, the major polymeric

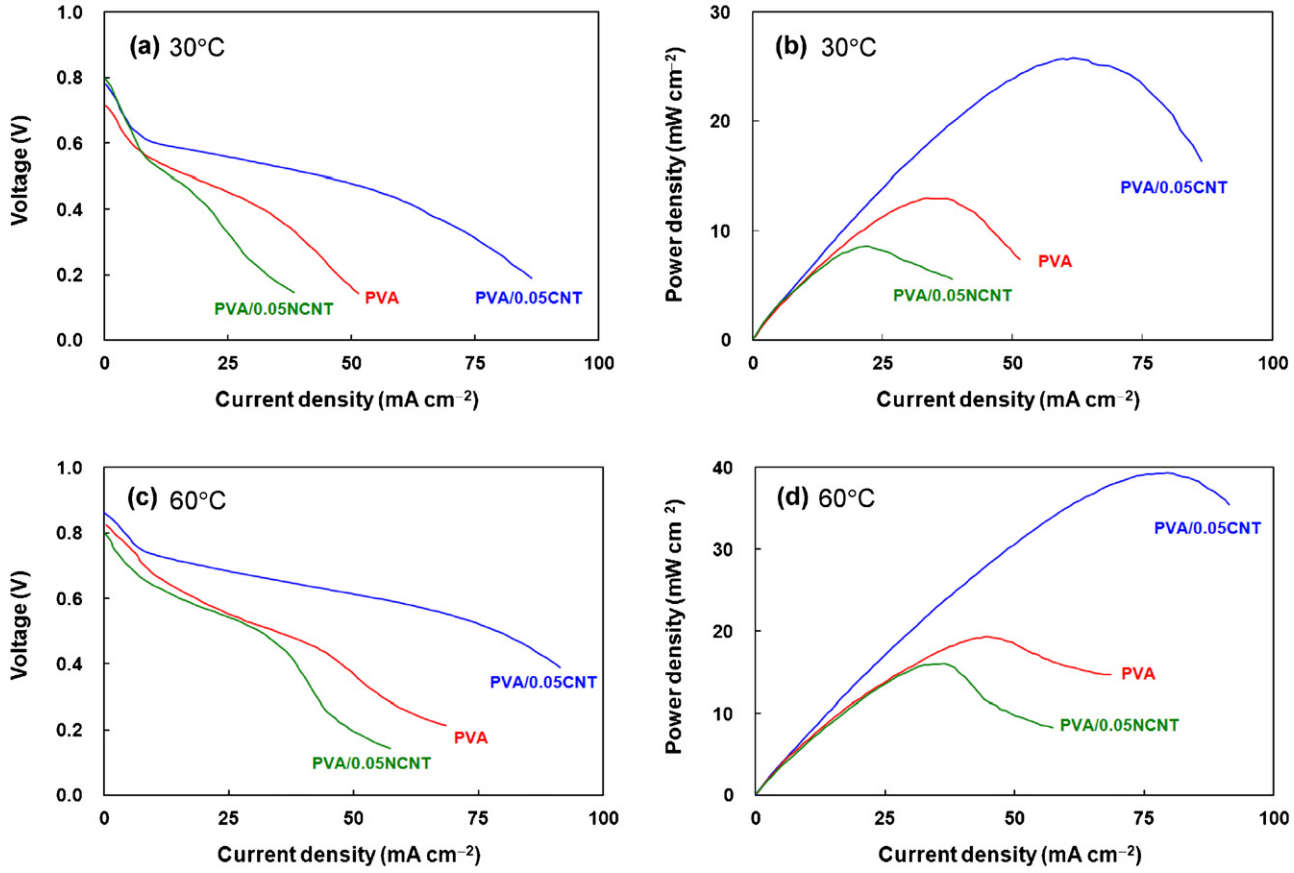

Fig. 3. (a, c) Voltage–current density and (b, d) power density–current density as a function of current density at 30 °C (a, b) and 60 °C (c, d) for DMAFCs using KOH-doped PVA, PVA containing 0.05% functionalized CNTs (PVA/0.05CNT), or PVA composite containing 0.05% nascent CNT (PVA/0.05NCNT) (anode: 2 M methanol in 6 M KOH at a flow rate of 5 mL min^{-1}, cathode: humidified oxygen at a flow rate of 100 mL min^{-1}).

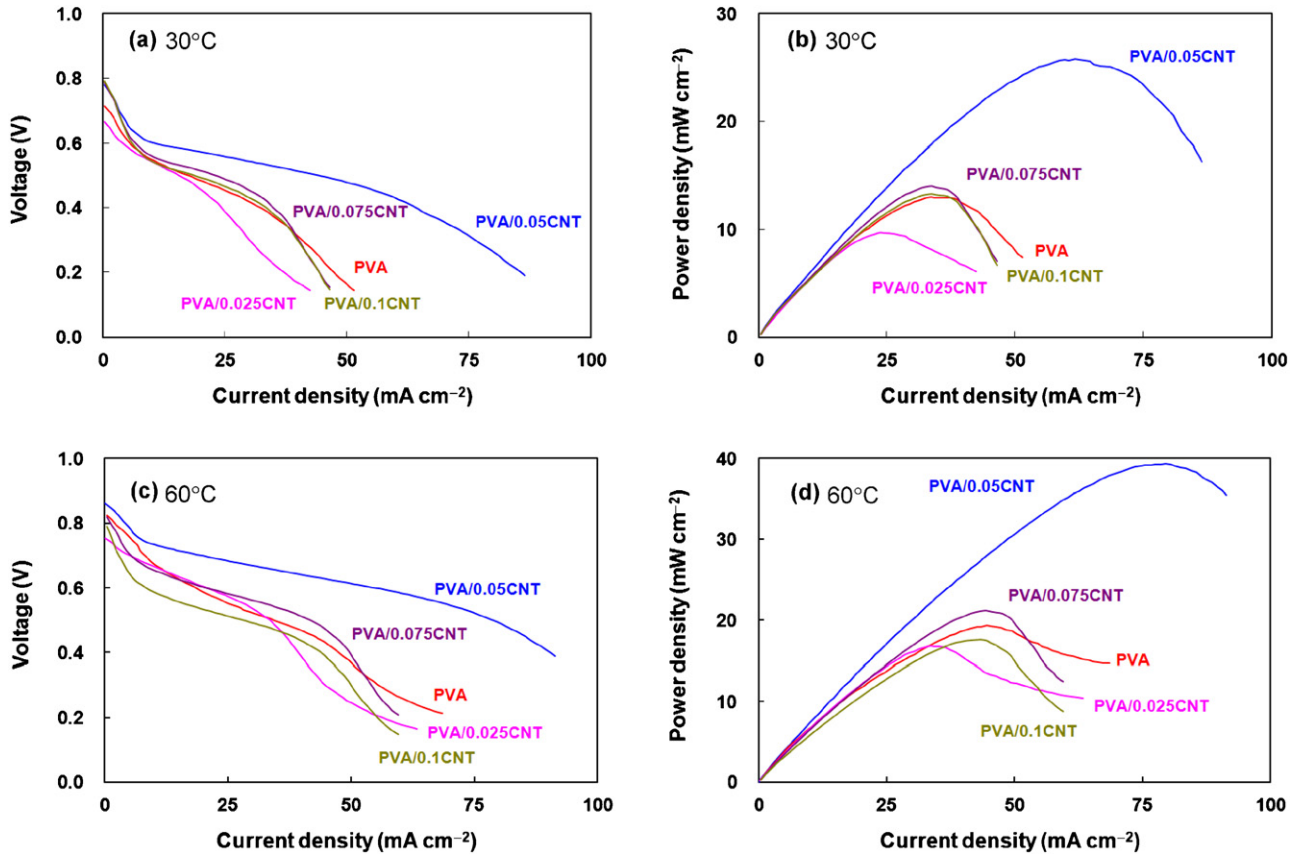

Fig. 4. Effect of CNT loading in electrolyte on DMAFC (a, c) voltage and (b, d) power density at (a, b) 30 °C and (c, d) 60 °C (anode: 2 M methanol in 6 M KOH with a flow rate of 5 mL min^{-1}, cathode: humidified oxygen with a flow rate of 100 mL min^{-1}).

component (PVA) in the PVA/CNT/KOH demonstrated a higher fractional free volume after wetting due to CNT addition, as shown in Fig. 1. The higher free volume significantly facilitates the transfer of hydroxide ions in the PVA/0.05CNT/KOH electrolyte membrane with respect to that in the PVA/KOH film. These results demonstrate that functionalized CNTs can achieve good compatibility with the PVA matrix, prevent electron leakage from the pristine NCNT, and increase the polymer free volume. These effects are advantageous for improving the full cell performance using the PVA/CNT composite rather than the PVA film.

3.4. Effect of CNT loading on cell performance

Various functionalized CNT loads were mixed with PVA to prepare PVA/CNT composites to evaluate DMAFC cell performance. Fig. 4 illustrates the cell performance at 30 and 60 °C. The 0.05% CNT-containing electrolyte exhibited the highest P_{max} among the tested samples. As the CNT load increased to 0.1%, the cell voltage and power density dropped significantly. Fig. 5 shows the P_{max} data as a function of the CNT load at 30 and 60 °C. In studying DMFC and PEMFC cell performance, Liu et al. found that 0.05% of Nafion®-functionalized CNTs and polybenzimidazole-functionalized CNTs produced higher performance than the other loads in the Nafion® matrix [34,38]. We also found that a 0.05% CNT loading produced the highest cell voltage and power density in the DMAFC in the 0–0.1% CNT range.

The effect of the CNT content on the cell performance can be explained in terms of the hydroxide transport in the polymer free volume and along the functionalized CNTs. As discussed in the previous section, the incorporation of 0.05% CNTs resulted in a higher free volume compared to the pristine PVA (Fig. 1). We also showed that the fractional free volume was positively related to water diffusivity and enhanced the hydroxide ion transfer through the PVA matrix [29]. Zhou et al. demonstrated that increasing CNT loading in a polymer matrix led to increased free volume. However, the free volume size was reduced beyond a specific level of CNT content [39] because the CNT tended to form aggregates and constrain molecular motion. As more CNTs were added to the polymer, the enhanced hydroxide ion transport in the CNT channel and the PVA matrix was offset by the more tortuous path in the CNT channel, the limited molecular chain motion, and the decreased free volume

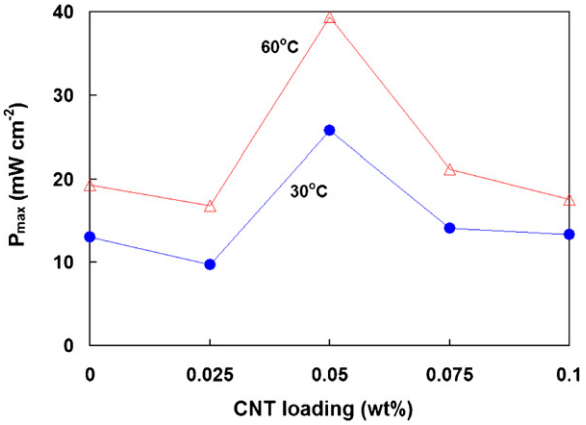

Fig. 5. P_{max} dependance on CNT loading in DMAFC electrolyte at 30 °C and 60 °C (anode: 2 M methanol in 6 M KOH with a flow rate of 5 mL min^{-1}, cathode: humidified oxygen with a flow rate of 100 mL min^{-1}).

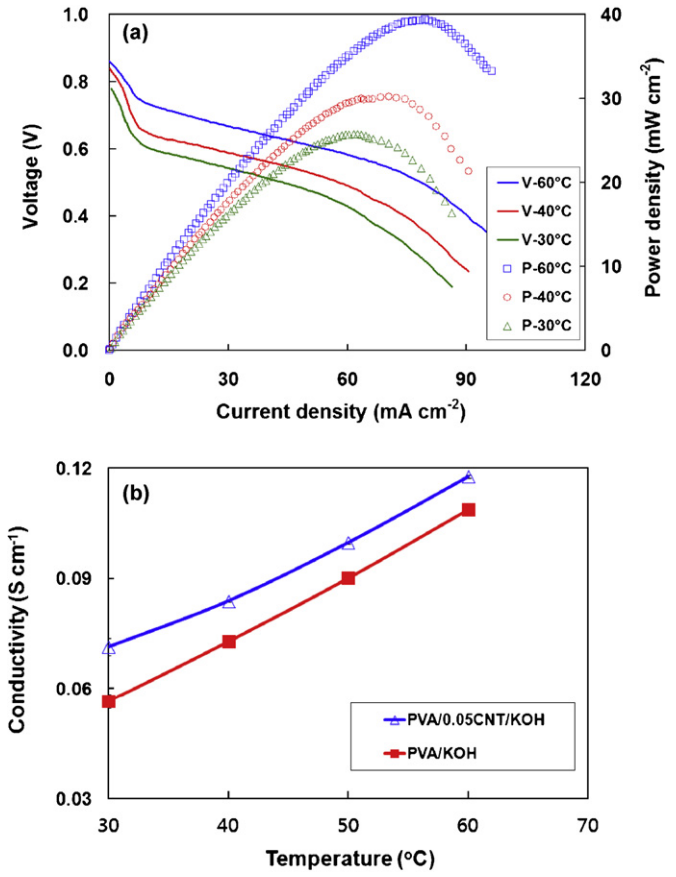

Fig. 6. Temperature effect on (a) DMAFC performance using PVA/0.05CNT/KOH electrolyte (anode: 2 M Methanol in 6 M KOH with a flow rate of 5 mL min^{-1}, cathode: humidified oxygen with a flow rate of 100 mL min^{-1}) and (b) ionic conductivity of PVA/0.05CNT/KOH electrolyte (doped in 6 M KOH).

(as presented in [39]) in the polymer matrix in the presence of the aggregated and poorly dispersed CNTs.

3.5. Temperature effect on cell performance

The cell voltage and power density data for the use of 2 M methanol and 6 M KOH, as the anode fuel, and the PVA/0.05CNT/KOH electrolyte at different temperatures (30–60 °C) are presented in Fig. 6. The V_{oc} increased with operating temperature. The P_{max} also increased at elevated temperatures. The P_{max} was 25.8, 30.1, and 39.4 mW cm^{-2} at 30, 40, and 60 °C, respectively.

A higher temperature results in the combined benefit of enhanced reaction rates at the electrodes [40,41] and less ohmic loss [7] in a single fuel cell. Both of these effects contribute to better cell performance. Increasing the temperature can accelerate the electrochemical kinetics of the oxidation reaction at the anode and the reduction reaction at the cathode. Therefore, the V_{oc} was enhanced at a higher temperature (Fig. 6(a)). The ionic conductivity of the PVA/CNT/KOH electrolyte was improved with increasing temperature, as shown in Fig. 6(b). The cell resistance decreased as the temperature was raised. A smaller ohmic over-potential was found at higher temperatures (Fig. 6(a)). Consequently, cell performance was improved due to faster electrochemical kinetic reaction rates and less electrical resistance in the fuel cell.

3.6. Methanol concentration effect on cell performance

The methanol concentration effect on the DMAFC performance was studied for a 1 M, 2 M, and 6 M anode feed. Fig. 7(a) shows the

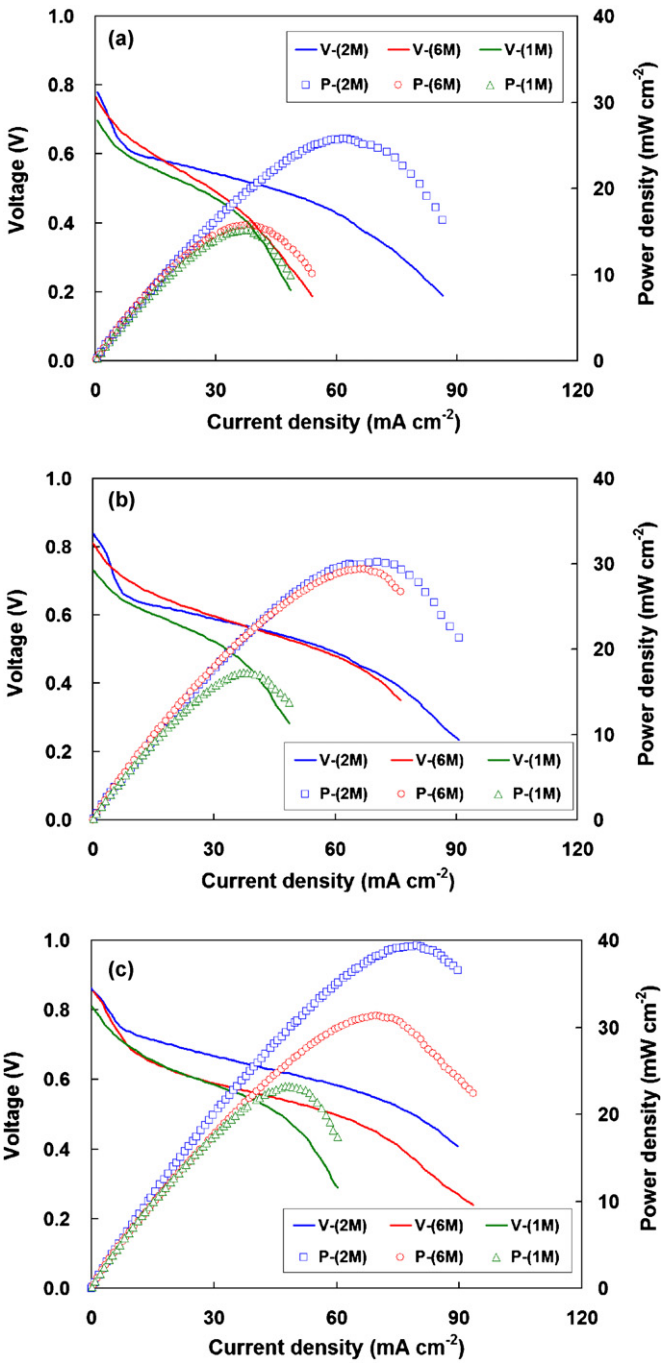

Fig. 7. Effect of methanol concentration on DMAFC cell performance with 6 M KOH at (a) 30 °C, (b) 40 °C, and (c) 60 °C (anode: methanol in 6 M KOH with a flow rate of 5 mL min^{-1}, cathode: humidified oxygen with a flow rate of 100 mL min^{-1}, electrolyte: PVA/0.05CNT/KOH).

voltage and power density values of the fuel cell at 30 °C. The P_{max} was 15.2, 25.8, and 15.6 mW cm^{-2} for the 1, 2, and 6 M methanol feed. As the temperature was increased to 40 °C, the P_{max} increased to 17.2, 30.1, and 29.4 mW cm^{-2} for the 1, 2, and 6 M methanol feeds, respectively (Fig. 7(b)). As the temperature reached 60 °C, the P_{max} reached 23.5, 39.4, and 31.1 mW cm^{-2} at these methanol concentrations (Fig. 7(c)).

The methanol oxidation rate is proportional to the square root of the methanol concentration in acid or alkaline medium [42,43]. The 2 M methanol concentration is more beneficial than the 1 M methanol concentration at 30 °C because the reaction rate favors a

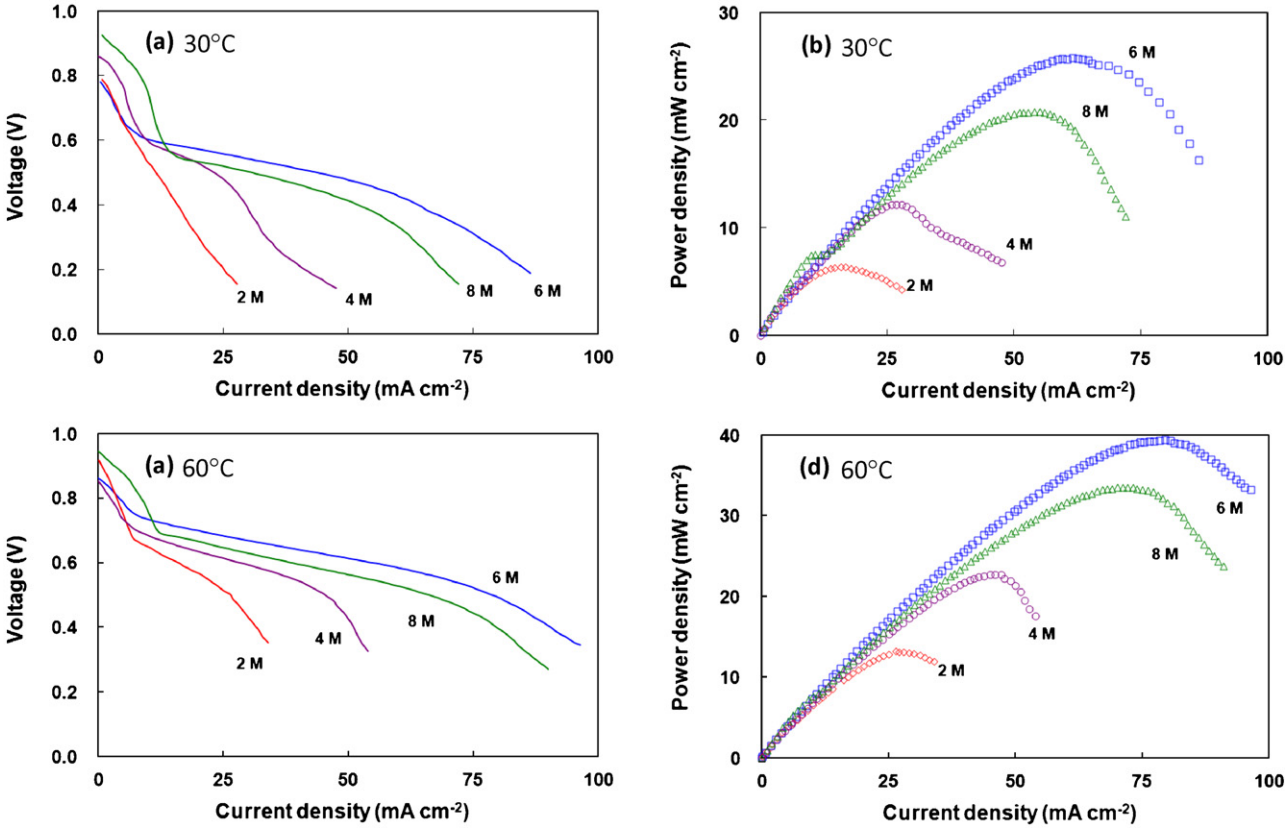

Fig. 8. Effect of KOH concentration on DMAFC (a, c) cell voltage and (b, d) power density at 30 °C (a, b) and 60 °C (c, d) (anode: 2 M methanol in KOH at a flow rate of 5 mL min^{-1}, cathode: humidified oxygen with a flow rate of 100 mL min^{-1}, electrolyte: PVA/0.05CNT/KOH).

higher fuel concentration. The 6 M methanol concentration of the anode fuel was not completely oxidized because of the low reaction kinetics at 30 °C. The un-reacted methanol then diffused to the cathode and caused a reduction in voltage due to a mixed cell potential at the cathode.

When the temperature was increased to 40 °C, the 2 M methanol fuel significantly outperformed the 1 M methanol fuel, which could not provide enough reactant to the anode. This reactant-limiting behavior was confirmed by the significantly lower P_{max} using 1 M methanol (17.2 mW cm^{-2}) with respect to the P_{max} for the 2 M methanol fuel (30.1 mW cm^{-2}). At 60 °C, both the 1 and 2 M methanol fuels resulted in even higher P_{max} values than 30 and 40 °C due to the higher reaction kinetics associated with 60 °C. Although the 6 M methanol fuel experienced an increase in P_{max} with respect to the values observed at 30 and 40 °C, this increase was limited (31.1 mW cm^{-2} and 29.4 mW cm^{-2} for 60 and 40 °C, respectively). This finding implies that the remaining, un-reacted methanol in the 6 M feed crossed over to the cathode and reduced the cell voltage. Many researchers have found that 2 M methanol produces higher cell voltages than other concentrations in DMFCs using a Nafion® electrolyte [1,44,45]. During the examination of the optimal methanol concentrations for DMAFCs and DMFCs, we observed several factors that governed the electrochemical behavior of the methanol fuel cell. The optimal methanol concentration is determined by the electrode reaction rates produced at a given cell temperature, anode electrode catalytic capacity, methanol permeability through the electrolyte membrane, and electrolyte thickness.

3.7. *Effect of KOH concentration on cell performance*

The DMAFC performance was evaluated in 2 – 8 M KOH with 2 M methanol fuel using the PVA/0.05CNT/KOH electrolyte. The same alkali concentration was used in doping the PVA composite electrolyte. The data are presented in Fig. 8. The V_{oc} ranged from 0.78 to 0.92 V at 30 °C (Fig. 8(a)) and 0.85 to 0.95 V at 60 °C (Fig. 8(c)). The P_{max} value was 6.4, 12.2, 25.8 and 20.8 mW cm^{-2} for 2, 4, 6, and 8 M KOH, respectively, at 30 °C (Fig. 8(b)) and 13.2, 22.7, 39.4, and 33.6 mW cm^{-2}, respectively, at 60 °C (Fig. 8(d)). The P_{max} appeared to increase proportionally with KOH concentration between 2 and 6 M but decrease at 8 M KOH.

Table 3
Resistance analysis of the membrane electrode assembly (MEA)[a] using different concentrations of KOH.

KOH concentration (M)	Resistance (MEA) (Ω)	Resistance (PVA/CNT/KOH electrolyte) (Ω)	Resistance (other)[b] (Ω)
4	0.895	0.248	0.652
6	0.583	0.128	0.452
8	0.686	0.169	0.511

[a] Electrolyte: PVA/0.05CNT/KOH, temperature: 60 °C.
[b] Resistance contributed from catalyst, gas diffusion layer, interface(s), graphite flow-field plates, and current collector. The value was estimated by subtracting the "Resistance (electrolyte)" values (experimental data using AC impedance spectroscopy) from the "Resistance (MEA)" values (data from the slopes of ohmic regions of *V–I* curves in Fig. 8(c)).

We have shown that the P_{max} of the DMAFC using PVA/fumed silica/KOH electrolyte linearly increased with KOH concentration in the 1–6 M range [7]. The higher KOH concentration in the anode fuel promotes the anode oxidation rate because it serves as the reactant at the anode [7]. The electrolyte doped with a high KOH concentration exhibited a higher conductivity than the low-concentration alkali [7,25]. Therefore, 6 M KOH produced higher cell performance than 1, 2, and 4 M alkali [7]. This study further confirms the notion that cell performance is enhanced by increasing the KOH concentration from 2 M to 6 M using the PVA/CNT/KOH electrolyte.

Increasing the KOH concentration to 8 M did not benefit the cell performance. In the low current density region (<12 mW cm^{-2}), the DMAFC using 8 M KOH generated the highest voltage among the cells. This finding may have been due to a higher anode reaction rate associated with the more concentrated KOH (one of the reactants on the anode) solution. As the current density increased, the cell voltage using 8 M KOH dropped more rapidly than the DMAFC with 6 M in the ohmic region (Fig. 8(a) and (c)). Almost all fuel cells operate in the ohmic region (the center straight line segment of the *V–I* curve), which merits more practical importance.

This higher power and cell voltage using 6 M KOH relative to using 8 M was due to the higher conductivity of the single cell made with 6 M KOH. The PVA electrolyte doped with 6 M KOH showed a higher conductivity than the 8 M KOH-doped electrolyte (0.12 vs. 0.10 S cm^{-1}). In addition, the specific conductivity of the 8 M KOH solution is not higher than that of the 6 M KOH solution [46,47], probably due to the higher solution viscosity and lower availability of free water for ionic conductance in the more concentrated KOH solution. The 8 M KOH might have caused a lower conductivity in the anode diffusion layer and interfaces and elevated the total cell resistance beyond that of the 6 M KOH solution, contributing to a higher overall cell resistance. This hypothesis is supported by our data. From the ohmic loss region, we observed a more profound voltage drop with the 8 M KOH solution than that using the 6 M KOH solution (0.68 V vs. 0.58 V per ampere increment, equivalent to 0.68 and 0.58 Ω), as determined from the segment slopes of the *V–I* curves. The PVA/0.05CNT/KOH electrolyte resistance data were obtained from the Nyquist plots of the AC impedance measurement. Then, the resistance, disregarding that of the electrolyte in the single cell, was calculated as the difference between the two sets of data and is summarized in Table 2. This measure (denoted as "Resistance (other)" in Table 3) comprises the resistances contributed from the catalyst, gas diffusion layers, the interfaces, etc. [7]. It is clear that the other resistance was the lowest for the 6 M KOH solution among 4–8 M KOH solutions (Table 3). Therefore, the P_{max} using 8 M KOH was lower than that using 6 M KOH (Fig. 8(b)).

3.8. Fuel and gas flow rate effect on cell performance

The oxygen flow rate may have controversial effects on cell performance. First, a higher oxygen flow rate implies more oxygen molecules are supplied to the cathode. This increase in oxygen molecules would benefit the oxygen reduction reaction at the cathode. Second, a higher gas flow rate may diminish the mass transport boundary layer surrounding the cathode catalyst and promote oxygen transport in this porous gas diffusion electrode. Finally, higher gas flow rates tend to remove water vapor from the fuel cell and dry the electrolyte. The oxygen flow rate was varied during the cell performance measurement in this study. Fig. 9 shows that cell performance declined when the oxygen flow rate was increased from 100 to 200 mL min^{-1} while the anode fuel flow rate was maintained at 5 mL min^{-1}. We observed that the higher gas flow rate dried out the electrolyte film and that the electrical resistance was increased, lowering the cell voltage and power density (Fig. 9).

Next the cathode gas flow rate was maintained at 100 mL min^{-1} for various anode feed flow rates, and the fuel cell was tested at 30 and 60 °C. At 30 °C, the P_{max} increased from 25.7 to 34.1 mW cm^{-2}, which corresponded to a 32.6% increase when the flow rate was increased from 5 to 30 mL min^{-1} (Fig. 10(a)). When the cell was operated at 60 °C, the P_{max} was improved from 39.3 to 68.1 mW cm^{-2} (73.2% increase) as the same anode flow rate increased (Fig. 10(b)).

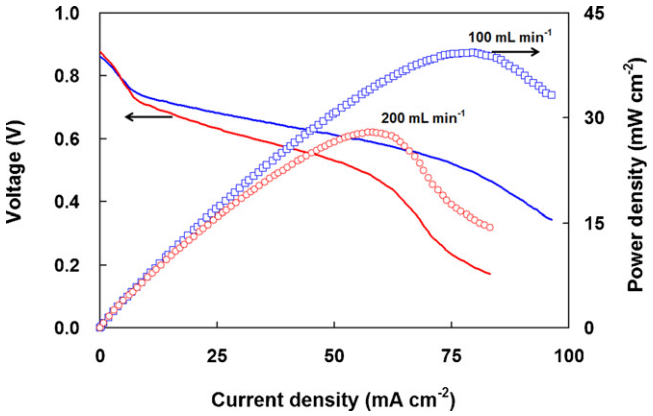

Fig. 9. Effect of cathode flow rate on DMAFC cell performance with PVA/0.05CNT electrolyte at 60 °C (anode: 2 M Methanol in 6 M KOH with a flow rate of 5 mL min^{-1}).

The fluid flow behavior can be expressed using a dimensionless parameter, the Reynolds number (Re). Anode feed flow rates of 5 and 30 mL min^{-1} corresponded to Re of 150 and 900, respectively, in the flow fields. Re is expected to increase in the gas diffusion layer [48]. The higher Re of the fuel is associated with a higher degree of turbulent flow. This turbulence helped reduce

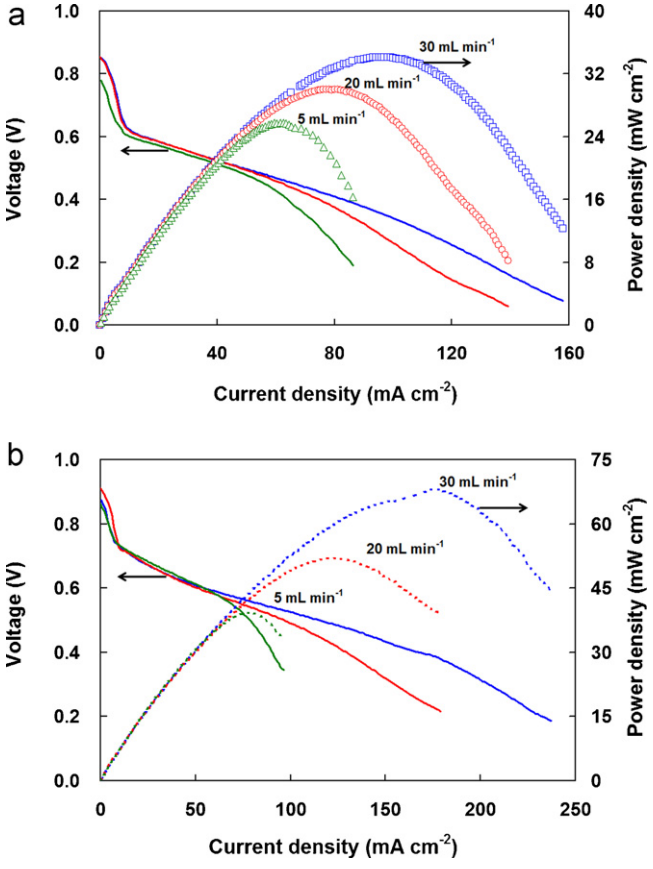

Fig. 10. Effect of anode flow rate on DMAFC cell performance with PVA/0.05CNT/KOH electrolyte at (a) 30 °C and (b) 60 °C (cathode: humidified oxygen at a flow rate of 100 mL min^{-1}).

Table 4
Comparison of peak power densities of DMAFCs reported in the literature (data sorted according to cell temperature, methanol and alkali concentrations).

Electrolyte	Operating conditions			Peak power density ($mW\,cm^{-2}$)	Source
	Anode catalyst (loading in $mg\,cm^{-2}$)	Temperature (°C)	Feed methanol concentration + alkali		
KOH-doped PVA/CNT	Pt–Ru (5)	60	2 M + 6 M KOH	68.1	This work
KOH-doped PVA/FS	Pt–Ru (5)	60	2 M + 6 M KOH	39	Lue et al. [7]
KOH-doped PVA/FS	Pt–Ru (5)	60	2 M + 2 M KOH	15.3	Lue et al. [7]
KOH-doped PVA crosslinked with sulfosuccinic acid	Pt–Ru (4.5)	60	2 M + 2 M KOH	4.13	Yang et al. [10]
KOH-doped PVA/TiO_2	Pt–Ru (4)	60	2 M + 2 M KOH	7.54	Yang [20]
KOH-doped PVA/FS	Pt–Ru (5)	60	2 M + 1 M KOH	7.9	Lue et al. [7]
KOH-doped PVA/CNT	Pt–Ru (5)	60	1 M + 6 M KOH	23.5	This work
KOH-doped PVA/FS	Pt–Ru (5)	60	1 M + 6 M KOH	30	Lue et al. [7]
KOH-doped PVA/FS	Pt–Ru (5)	60	1 M + 1 M KOH	10.2	Lue et al. [7]
KOH-doped PVA/CNT	Pt–Ru (5)	40	6 M + 6 M KOH	29.4	This work
KOH-doped PVA/CNT	Pt–Ru (5)	40	2 M + 6 M KOH	30.1	This work
KOH-doped PVA/FS	Pt–Ru (5)	40	2 M + 6 M KOH	30	Lue et al. [7]
KOH-doped PVA/CNT	Pt–Ru (5)	30	2 M + 6 M KOH	25.8	This work
KOH-doped PVA/FS	Pt–Ru (5)	30	2 M + 6 M KOH	15	Lue et al. [7]

the methanol concentration polarization in the boundary layer surrounding the catalyst and promoted methanol transport from the feed solution to the active catalytic sites. The turbulence could also remove the produced CO_2 gas from the catalyst surface to the bulk solution. This CO_2 gas removal was especially beneficial at 60 °C because more CO_2 gas was generated at this temperature than at 30 °C. These DMAFC cell performance data were compared with the literature data and are shown in Table 4, grouped according to the dominant operating parameters. Please note that the peak power density data were generated under various operating conditions. The results are better compared under similar test conditions (with some critical parameters shown in Table 4). For instance, we can compare results at 60 °C, 1–2 M methanol concentration, and 4–5 $mg\,cm^{-2}$ catalyst loading. Yang et al. [10,20] obtained peak power densities of 4.13 and 7.54 $mW\,cm^{-2}$ using KOH-doped cross-linked PVA and PVA/TiO_2 electrolytes, respectively, at 60 °C with 2 M methanol and 2 M KOH as the anode feed. Even with a cell operated at 30 °C using this PVA/0.05CNT/KOH electrolyte, we could obtain a P_{max} (25.8 $mW\,cm^{-2}$) higher than those reported for 50 °C by Matsuoka et al. [6] (6.1 $mW\,cm^{-2}$ with a hydrocarbon-based anion exchange membrane using 1 M methanol and 1 M KOH as the anode feed) and Varcoe et al. [16] (2.1 $mW\,cm^{-2}$ using a poly(ethylene-*co*-tetrafluoroethylene)-derived anion exchange membrane and 2 M methanol fuel). The electrochemical results in this study are superior to these reported in the literature. The PVA/0.05CNT/KOH electrolyte produced the highest P_{max} values in all groups under similar tested temperatures (Table 4). We achieved a P_{max} of 68 $mW\,cm^{-2}$ using the PVA/0.05CNT/KOH electrolyte under the optimal operating condition. This P_{max} value is the highest result reported in the DMAFC literature to the best of our knowledge. This value approaches the observed in DMFCs using a Nafion® membrane under the proton-exchange mode at 60 °C [49].

4. Conclusion

The PVA/CNT/KOH electrolyte has a great potential for DMAFC applications. The optimal CNT load was found to be 0.05%. DMAFCs using the PVA/0.05CNT/KOH electrolyte were evaluated under various operating conditions. The results indicate that the temperature, methanol and KOH solution concentrations, and fuel flow rate were the key operating parameters that influence the DMAFC performance. An open-circuit potential and a peak power density of 0.87 V and 68.1 $mW\,cm^{-2}$, respectively, were obtained using a 2 M methanol fuel in 6 M KOH with a flow rate of 30 $mL\,min^{-1}$ and humidified oxygen fed at 100 $mL\,min^{-1}$ at 60 °C. The P_{max} achieved is the highest among values reported in the DMAFC literature under comparable operating conditions.

Acknowledgements

We thank the National Science Council of Taiwan for financial support (NSC 98-2221-E-182-034) and Mr. K.S. Liao at R&D Center for Membrane Technology of Chung Yuan University for PALS analysis. The valuable discussions from the referees are greatly acknowledged.

References

[1] S. Mollá, V. Compañ, J. Power Sources 196 (2011) 2699–2708.
[2] H.C. Cha, C.Y. Chen, J.Y. Shiu, J. Power Sources 192 (2009) 451–456.
[3] V. Neburchilov, J. Martin, H. Wang, J. Zhang, J. Power Sources 169 (2007) 221–238.
[4] J. Kim, T. Momma, T. Osaka, J. Power Sources 189 (2009) 999–1002.
[5] E.H. Yu, K. Scott, J. Power Sources 137 (2004) 248–256.
[6] K. Matsuoka, Y. Iriyama, T. Abe, M. Matsuoka, Z. Ogumi, J. Power Sources 150 (2005) 27–31.
[7] S.J. Lue, W.T. Wang, K.P.O. Mahesh, C.C. Yang, J. Power Sources 195 (2010) 7991–7999.
[8] S.J. Lue, K.P.O. Mahesh, W.T. Wang, J.Y. Chen, C.C. Yang, J. Membr. Sci. 367 (2011) 256–264.
[9] C.C. Yang, S.J. Chiu, W.C. Chien, S.S. Chiu, J. Power Sources 195 (2010) 2212–2219.
[10] C.C. Yang, S.J. Chiu, W.C. Chien, J. Power Sources 162 (2006) 21–29.
[11] E.H. Yu, U. Krewer, K. Scott, Energies 3 (2010) 1499–1528.
[12] Y. Chen, L. Zhuang, J. Lu, Chin. J. Catal. 28 (2007) 870–874.
[13] E.H. Yu, K. Scott, J. Appl. Electrochem. 35 (2005) 91–96.
[14] E.H. Yu, K. Scott, R.W. Reeve, J. Appl. Electrochem. 36 (2006) 25–32.
[15] K. Scott, E.H. Yu, G. Vlachogiannopoulosa, M. Shivare, N. Duteanu, J. Power Sources 175 (2008) 452–457.
[16] J.R. Varcoe, R.C.T. Slade, E.L.H. Yee, S.D. Poynton, D.J. Driscoll, D.C. Apperley, Chem. Mater. 19 (2007) 2686–2693.
[17] C. Coutanceau, L. Demarconnay, C. Lamy, J.M. Leger, J. Power Sources 156 (2006) 14–19.
[18] J.H. Kim, H.K. Kim, K.T. Hwang, J.Y. Lee, Int. J. Hydrogen Energy 35 (2010) 768–773.
[19] H. Hou, G. Sun, R. He, B. Sun, W. Jin, H. Liu, Q. Xin, Int. J. Hydrogen Energy 33 (2008) 7172–7176.
[20] C.C. Yang, J. Membr. Sci. 288 (2007) 51–60.
[21] C.C. Yang, S.J. Chiu, C.T. Lin, J. Power Sources 177 (2008) 40–49.
[22] C.C. Yang, S.J. Chiu, K.T. Lee, W.C. Chien, C.T. Lin, C.A. Huang, J. Power Sources 184 (2008) 44–51.
[23] J. Fu, J. Qiao, X. Wang, J. Ma, T. Okada, Synth. Met. 160 (2010) 193–199.
[24] W.H. Pan, S.J. Lue, C.M. Chang, Y.L. Liu, J. Membr. Sci. 376 (2011) 225–232.
[25] Y. Zhang, Z. Cui, C. Liu, W. Xing, J. Zhang, J. Power Sources 194 (2009) 730–736.
[26] C.C. Yang, W.C. Chien, Y.J. Li, J. Power Sources 195 (2010) 3407–3415.
[27] E. Muñoz, A.B. Dolton, S. Collins, M. Kozlov, J. Razal, J.N. Coleman, B.G. Kim, V.H. Ebron, M. Selvidge, J.P. Ferraris, R.H. Baughman, Adv. Eng. Mater. 6 (2004) 801–804.

[28] S.J. Ewing, R. Lan, X.X. Xu, S.W. Tao, Fuel Cells 10 (2010) 72–76.
[29] S.J. Lue, D.T. Lee, J.Y. Chen, C.H. Chiu, C.C. Hu, Y.C. Jean, J.Y. Lai, J. Membr. Sci. 325 (2008) 831–839.
[30] R. Kannan, B.A. Kakade, V.K. Pillai, Angew. Chem. Int. Ed. 47 (2008) 2653–2656.
[31] R. Kannan, M. Parthasarathy, S.U. Maraveedu, S. Kurungot, V.K. Pillai, Langmuir 25 (2009) 8299–8305.
[32] Y.L. Liu, W.H. Chen, Y.H. Chang, Carbohydr. Polym. 76 (2009) 232–238.
[33] C.M. Chang, Y.L. Liu, Carbon 48 (2010) 1289–1297.
[34] Y.L. Liu, Y.H. Su, C.M. Chang, Suryani, D.M. Wang, J.Y. Lai, J. Mater. Chem 20 (2010) 4409–4416.
[35] S.J. Lue, J.Y. Chen, J.M. Yang, J. Macromol. Sci. Phys. 47 (2008) 39–51.
[36] S. Frank, P. Poncharal, Z.L. Wang, W.A. de Heer, Science 280 (1998) 1744–1746.
[37] K. Matsumoto, T. Fujigaya, H. Yanagi, N. Nakashima, Adv. Funct. Mater. 21 (2011) 1089–1094.
[38] Suryani, C.M. Chang, Y.L. Liu, Y.M. Lee, J. Mater. Chem. 21 (2011) 7480–7486.
[39] W. Zhou, J. Wang, Z. Gong, J. Gong, N. Qi, B. Wang, Appl. Phys. Lett. 94 (2009), 021904-1-021904-3.
[40] E.H. Yu, K. Scott, R.W. Reeve, J. Electroanal. Chem. 547 (2003) 17–24.
[41] M. Uma, R. Manoharan, Bull. Electrochem. 12 (1996) 196–200.
[42] S.Lj. Gojković, T.R. Vidaković, D.R Đurović, Electrochim. Acta 48 (2003) 3607–3614.
[43] A.V. Tripković, K.D.J. Popović, J.D. Lović, J. Serb. Chem. Soc. 72 (2007) 1095–1101.
[44] D.H. Jung, C.H. Lee, C.S. Kim, D.R. Shin, J. Power Sources 71 (1998) 169–173.
[45] J. Ge, H. Liu, J. Power Sources 142 (2005) 56–69.
[46] R.J. Guanti, P.J. Moran, J. Appl. Electrochem. 16 (1986) 678–682.
[47] W. Pyle, J. Healy, R. Cortez, Home Power 39 (1994) 32–38.
[48] J.G. Pharoah, Int. J. Green Eng. 2 (2005) 421–438.
[49] B. Gurau, E.S. Smotkin, J. Power Sources 112 (2002) 339–352.